SPIE Smart Structures and Materials Conference 2006, San Diego, CA
SPIE Paper #6172-40, Tracking #SS06-SSM07-9

Nano-interconnection for microelectronics and polymers with benzo-triazole

Yeonjoon Park[1], Sang H. Choi[2], Hyunpil Noh[3], and Young Kuk[4]

[1] Science and Technology Corp., Hampton, VA
[2] NASA Langley Research Center, Hampton, VA
[3] Samsung Electronics Co. Ltd., Seoul, Korea
[4] Dept. of Physics, Seoul National University, Seoul, Korea

Abstract

Benzo-Triazole (BTA) is considered as an important bridging material that can connect an organic polymer to the metal electrode on silicon wafers as a part of the microelectronics fabrication technology. We report a detailed process of surface induced 3-D polymerization of BTA on the Cu electrode material which was measured with the Ultraviolet Photoemission Spectroscopy (UPS), X-ray Photoemission Spectroscopy (XPS), and Scanning Tunneling Microscope (STM). The electric utilization of shield and chain polymerization of BTA on Cu surface is contemplated in this study.

Introduction

It is an exciting and important challenge to fabricate an IC chip that can be connected to bio-materials, proteins, tissues, or neurons. In order to achieve this goal, the current nano-electronics requires certain bridge-materials that can connect the metal electrodes to the organic polymers. For example, a small fiber-fragment fails to connect two Au electrodes in Figure 1-(a). If there existed a certain bridge-material that can grab the metal electrode and fiber-fragment at the same time, current-voltage (I-V) characteristics of the fiber could be obtained in this micro circuit. As another example, Figure 1-(b)~(d) show the manipulation of bio-protein, Ferritin with Atomic Force Microscope (AFM) tip. Ferritin is an important protein that stores the iron ions inside the hemoglobin of the blood cell.[i, ii] Randomly distributed ferritin proteins were brought together to build a compact nano structure. The entire AFM manipulation took place inside a junction area of metal electrodes on a micro-chip, as shown in Figure 1-(e), (f), and (g). However, the final interconnections from the nearby metal electrodes to the arranged ferritin proteins are still missing. Therefore it is important to develop good materials that can act as a bridge between metal electrodes and bio proteins, organic polymers, and nano structures.

The common metal electrodes of Integrated Circuit (IC) chips are made with aluminum (Al), tungsten (W), gold (Au) and copper (Cu).[iii] Among these metals, Cu has extremely large diffusion-coefficient[iv] in silicon wafer and it often destroys many transistors. Therefore, Cu was accepted as an electrode material in the silicon technology, only after the diffusion problems were solved with Damascene process developed by IBM.[iii, v]

Benzotriazole (BTA) is an interesting molecule that is known to polymerize on Cu surface and form a protective layer against oxidation and etching of Cu electrodes and yet to be very conductive in the thin film thickness. Therefore, we report the detailed polymerization process of BTA[vi] once more in this conference and suggest the utilization of BTA to interconnect external organic polymers to the metal electrodes by functionalization of BTA molecules.

Experiment and Results

BTA is an organic molecule with a hexagonal benzene ring and pentagonal nitrogen ring as shown in Figure 2. Various different surface polymerization models have been proposed by many groups as shown in Figure 2. Roberts and Rubim et al.[vii] suggested a flat surface adsorption while Boshung Fang et al.[viii] suggested a vertical polymerization with nitrogen-hydrogen bond. Zhi Xu et al. measured the tilted angle of symmetric axis of BTA to be 62° with dichroic ratio measurement, in an effort to support the vertical polymerization model.[ix] Walsh et al.[x] suggested a vertical adsorption model of BTA on Cu(100) surface from a polarization dependent NEXAFS study. However, no clear conclusion has been made among these numerous studies.

BTA is known to have complex molecular orbitals as shown in Table 1. Molecular orbital (MO) P1~P5 are π–MOs with anti symmetric property upon the central plane and S1~S5 are σ–MOs with symmetric property upon the central

plane. N+ and N- states are the nitrogen induced states. Note that P1 and P2 are hybrid π-MOs while P3, P4 and P5 are global π–MO.

MO Name	Ionization Energy (eV)	Orbital Assignment	MO Name	Ionization Energy(eV)	Orbital Assignment
P5	9.08	π	S5	13.30	σ
P4	9.49	π	P1	15.02	π,σ,σ,σ
N-	10.05	N-	S4	16.93	σ
P3	11.44	π	S3	17.67	σ
N+	11.93	N+	S2	19.60	σ,σ
P2	12.77	π,σ	S1	20.10	σ

Table 1-Molecular Orbitals of BTA[viii, xi]

In our experiment, BTA was evaporated in ultra high vacuum chamber to be deposited on Cu(110) single crystal. The Cu(110) single crystal was cleaned with repeated Ar sputtering and annealing at 550°C. Before the deposition, a sharp (1x1) reconstruction was confirmed with Low Energy Electron Diffraction (LEED). Additional X-ray Photoemission Spectroscopy (XPS) was taken to confirm the cleanness of Cu surface. Using the LEED, UV source was aligned 10° off from the surface tangential direction toward [002] orientation of Cu(110) crystal in order to detect surface sate at $\overline{Y}$ direction. The UV detector was aligned 20° off from the surface normal direction. Unpolarized He(I) 21.2eV light was used as the UV source. After the above setup, Ultraviolet Photoemission Spectroscopy (UPS) data was collected as a function of the BTA deposition time into the UHV chamber. The deposition time was controlled with a gate valve. Since the vapor pressure of BTA is $8\text{x}10^{-6}$ torr at 300K, the evaporation of BTA occurred even at room temperature. The base pressure of UPS chamber was $2.0\text{x}10^{-10}$ torr and the pressure was raised by $4\text{x}10^{-10}$ torr during the deposition.

Figure 3-(a) shows the UPS data from clean Cu surface to 80 min. after of BTA deposit and Figure 3-(b) shows the data portion from 80 min. to 230 min. of BTA deposit. In the beginning Cu 3d band peaks are dominant, but BTA peaks start to appear and become stronger as more deposition occurs after 80 min. In Figure 3-(a), the most prominent peak is labeled as "Initial Growth Peak" which was identified as BTA's P3 molecular orbital. At 230min. of BTA deposit, all the peaks, S4, P1, S5, P2, N+ and P3, can be identified as shown in Figure 3-(b). Figure 4 shows the net peak intensity of 80 min. despot and 230 min. deposit without the Cu background signal. Interestingly in the initial deposit of 80 min., P3 was the strongest but P3 becomes weaker after 80 min. when it is compared with other peaks at a later stage of deposit.

Figure 5-(A) shows the change in relative intensity when each peak intensity at 230 min. deposit is taken as 100%. Obviously, the global π–molecular orbital P3 takes a different trend-[1] of intensity growth while all other peaks follow the common trend-[2]. To understand this awkward phenomenon, we proposed an ab-initio calculation model in which BTA molecule changes its orientation depending on the deposit thickness since this model can explain the UPS intensity change of P3 MO.

Generally, the intensity of detected electrons in photoemission spectroscopy is proportional to the differential cross-section, $\frac{d\sigma}{d\Omega}$ of the sample, BTA, such as;

$$\frac{d\sigma}{d\Omega} = \frac{\alpha}{\pi}\frac{k}{\omega}\left|\left\langle f\left|\hat{A}\cdot\vec{p}\right|i\right\rangle\right|^2 \cdot a_0^2$$

where k and ω are wave-number and angular frequency of the light, $\hat{A}$ is the polarization direction and also the vector potential direction of the light.

With the dipole approximation, $\hat{A}\cdot\left\langle f\left|\vec{p}\right|i\right\rangle = im\omega_{fi}\hat{A}\cdot\left\langle f\left|\vec{x}\right|i\right\rangle$

Therefore the intensity is determined by

$$\hat{A}\cdot\left\langle f\left|\vec{p}\right|i\right\rangle = \oint\left\{\left(\hat{A}\cdot\vec{x}\right)\Psi_f^*(\vec{x})\Psi_i(\vec{x})\right\}d^3\vec{x}$$ ----------*Eq.(A)*

The P3 global π–molecular orbital has anti-symmetric property as shown in Figure 5-(B)-(a). Now, a total of six different cases can be considered with the polarization directions and BTA's positions. Four of the six cases are shown

in Figure 5-(B)-(b) to Figure 5-(B)-(e), that are consistent with our experiment. In UPS, the final state can be approximated with a parallel traveling electron wave-function in z-direction, $\propto e^{ikz}$. In the case of Near Edge X-ray Absorption Fine Structure (NEXAFS) or X-ray Absorption Near-Edge Structure (XANES), the final state is the unoccupied excited molecular orbital.

Case (1): BTA adsorbed flat on Cu and the light's polarization is parallel with surface, as shown in Figure 5-(B)-(b)

$$Eq.(A) = 2\int d\rho \int d\phi \int_0^{\infty} dz \rho z \Psi_i(\rho,\phi,z)\cos(kz) = \text{non} - \text{zero strong intensity}$$

Case (2): BTA adsorbed flat on Cu and the light's polarization is vertical to the surface, as shown in Figure 5-(B)-(c)

$$Eq.(A) = -2i\int d\rho \int d\phi \int_0^{\infty} dz \rho^2 \cos(\phi)\sin(kz)\Psi_i(\rho,\phi,z) = \text{non} - \text{zero strong intensity}$$

Case (3): BTA stands up, facing the light's propagation and the light's polarization is vertical to the surface, as shown in Figure 5-(B)-(d)

$$Eq.(A) = \int d\rho \int dz \int_0^{\pi} d\phi \rho z e^{-ikz}\Psi_i(\rho,\phi,z) + \int d\rho \int dz \int_{-\pi}^{0} d\phi \rho z e^{-ikz}\Psi_i(\rho,\phi,z) = 0$$

, due to the anti-symmetric property of $\Psi_i(\rho,\phi,z)$, the global π–molecular orbital P3.

Case (4): BTA stands up, facing the light's propagation and the light's polarization is parallel with the surface, as shown in Figure 5-(B)-(e)

$$Eq.(A) = \int d\rho \int dz \int_0^{\pi} d\phi \rho^2 \cos(\phi) e^{-ikz}\Psi_i(\rho,\phi,z) + \int d\rho \int dz \int_{-\pi}^{0} d\phi \rho^2 \cos(\phi) e^{-ikz}\Psi_i(\rho,\phi,z) = 0$$, due to the anti-symmetric property of $\Psi_i(\rho,\phi,z)$, the global π–molecular orbital P3.

By summarizing the above four cases when BTA adsorbs flat on Cu surface, UPS intensity of P3 is strong with non-zero term in equation (A) regardless of polarization direction such as non-polarized UV source. On the other hand, when BTA stands up on Cu surface facing the light propagation, the UPS intensity is very weak with zero term in equation (A). This kind of symmetry argument is very useful to determine the molecular orientation and can be expanded to NEXAFS and XANES as well as UPS.

Our model explains the behavior of P3's UPS intensity in Figure 5-(a). Therefore, we conclude that BTA adsorbs flat on Cu surface in the beginning, but vertical BTA molecules appear at higher concentration and form polymerization. However, we could not determine whether the vertical polymerization occurs at one monolayer with higher coverage or it occurs at the 2nd monolayer and above. Another separate Scanning Tunneling Microscope (STM) measurement[xii] was made by Dr. Keyhyun Cho, as shown in Figure 6. STM image confirms flat adsorbed BTA and vertically oriented polymerized BTA's chain. Therefore, we suggest a new polymerization model that BTA makes flat absorption like shields on Cu surface first, and then makes vertically oriented polymerization like a chain that binds shields or fills space between shields to protect Cu surface. This property is very important and useful for a fabrication of a micro-chip that can connect organic polymers and bio materials because BTA can grab the Cu atoms on the surface with strong π–bond and capture external organic polymers with their polymer chains.

Summary

We measured thickness dependent UPS data of BTA on Cu(110) surface. Our theoretical model based on the symmetry property of P3 molecular orbital indicates that BTA changed molecular orientation during deposition. The developed symmetry calculation method is very general and can be also expanded to NEXAFS and XANES. The measured

polymerization process of BTA shows that BTA is a good candidate material that can anchor external organic molecules on Cu electrodes in microelectronics fabrication process.

Acknowledgement

This presentation was supported by Creativity and Innovation Program of NASA Langley Research Center. The authors appreciate Dr. Jaewoo Kim at STC, Hampton, VA for AFM data and Dr. Keyhyun Cho at Yeungnam University, South Korea who studied BTA molecules with STM and assisted us.

Figures

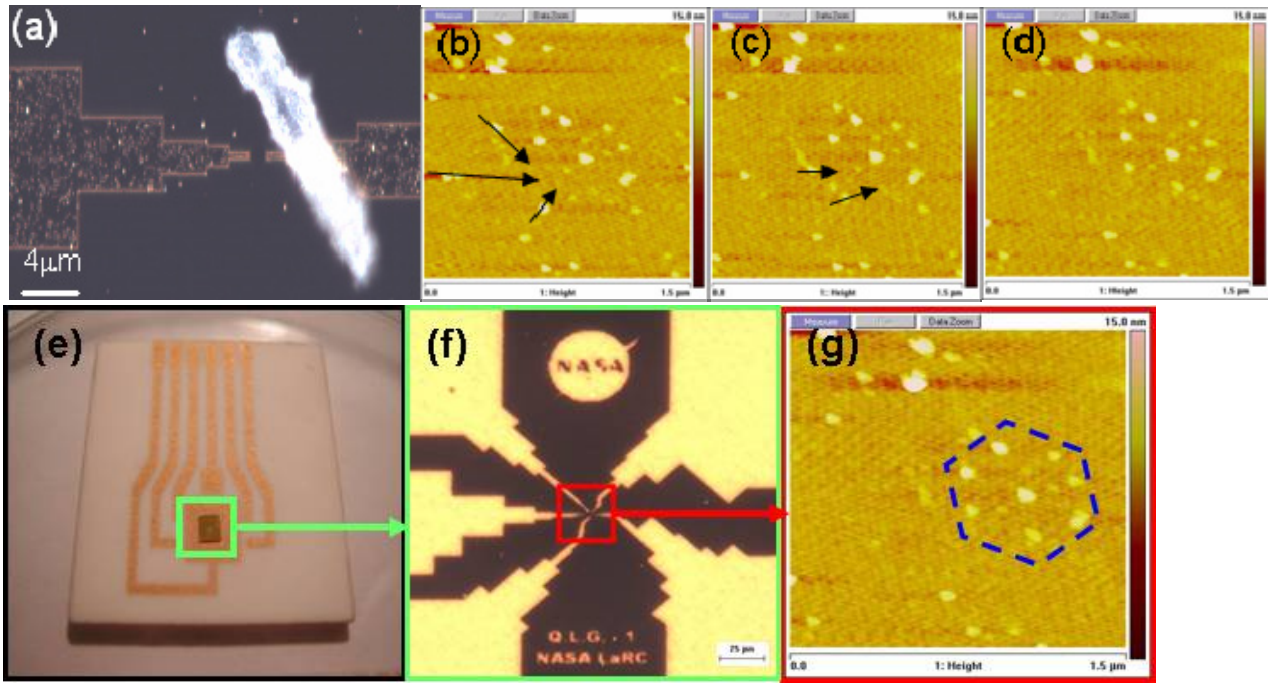

Figure 1 - (a) Interconnection failure of polymer structure to Au electrodes, (b)~(d) Manipulation of bio-protein , Ferritins with AFM tip: the arrow shows the motion of Ferritins as a result of AFM tip manipulation, (e) microchip in a few cm size, (f) metal electrode area in the microchip, (g) arranged Ferritin proteins in the center of electrode junction point. The interconnections to these proteins are still missing.

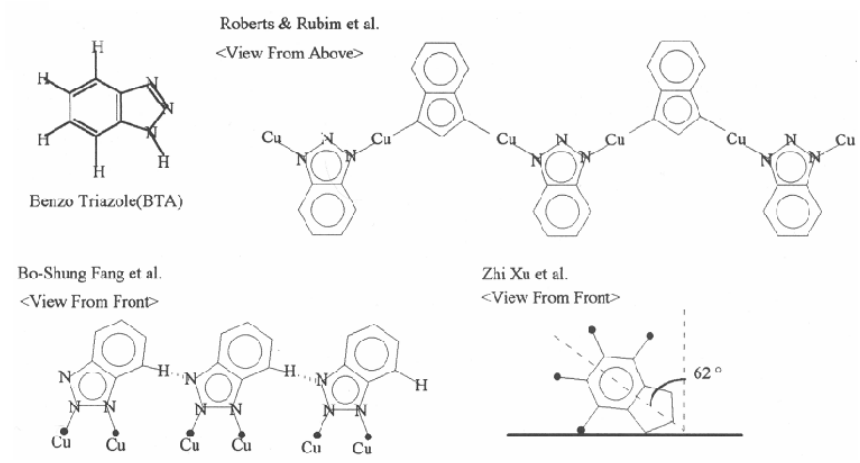

Figure 2 - BTA molecular structure and previously suggested adsorption models on Cu surface

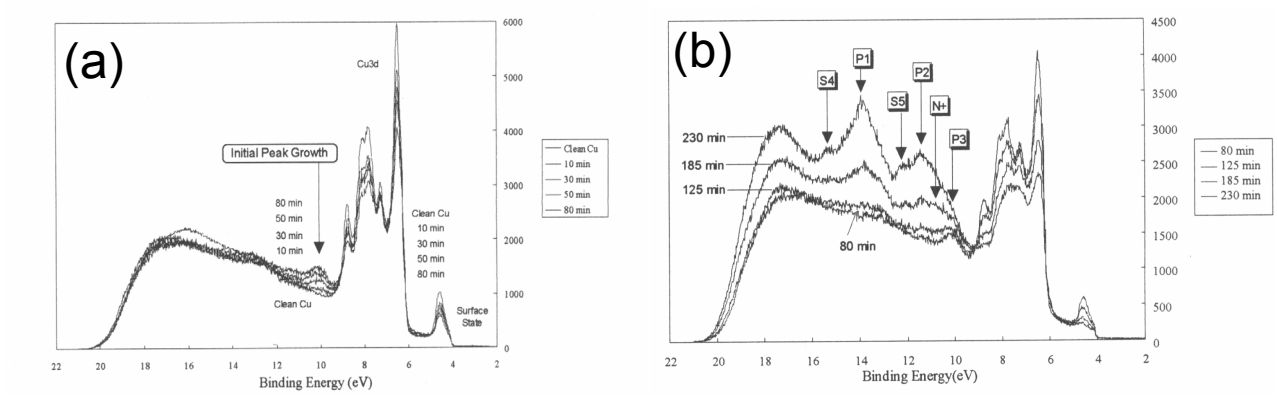

Figure 3 - (a) UPS data of BTA deposit up to 80 min., (b) UPS data of BTA deposit from 80 min. to 230 min.

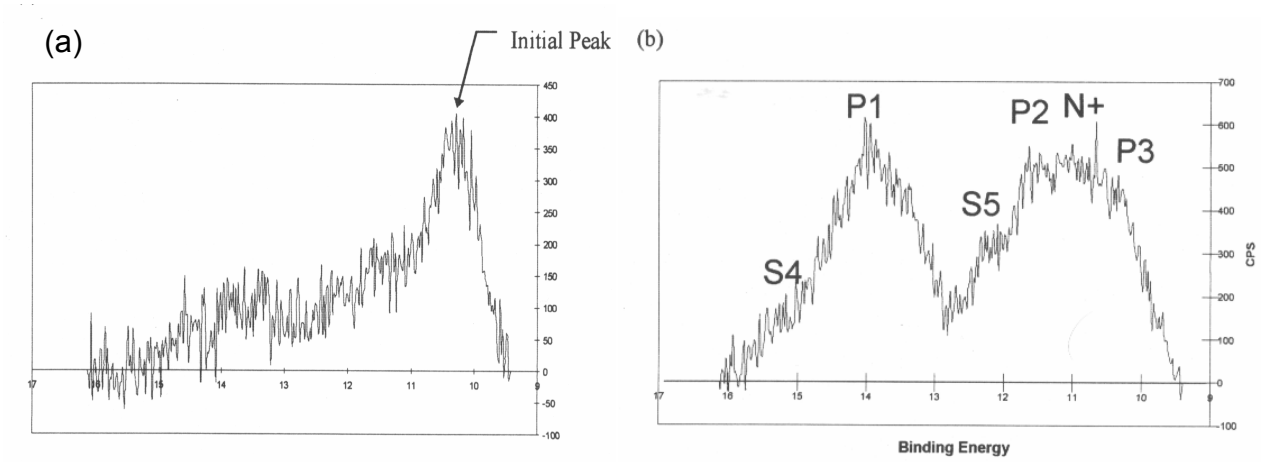

Figure 4 - Comparison of UPS data of BTA deposit between (a) 80 min. and (b) 230 min.

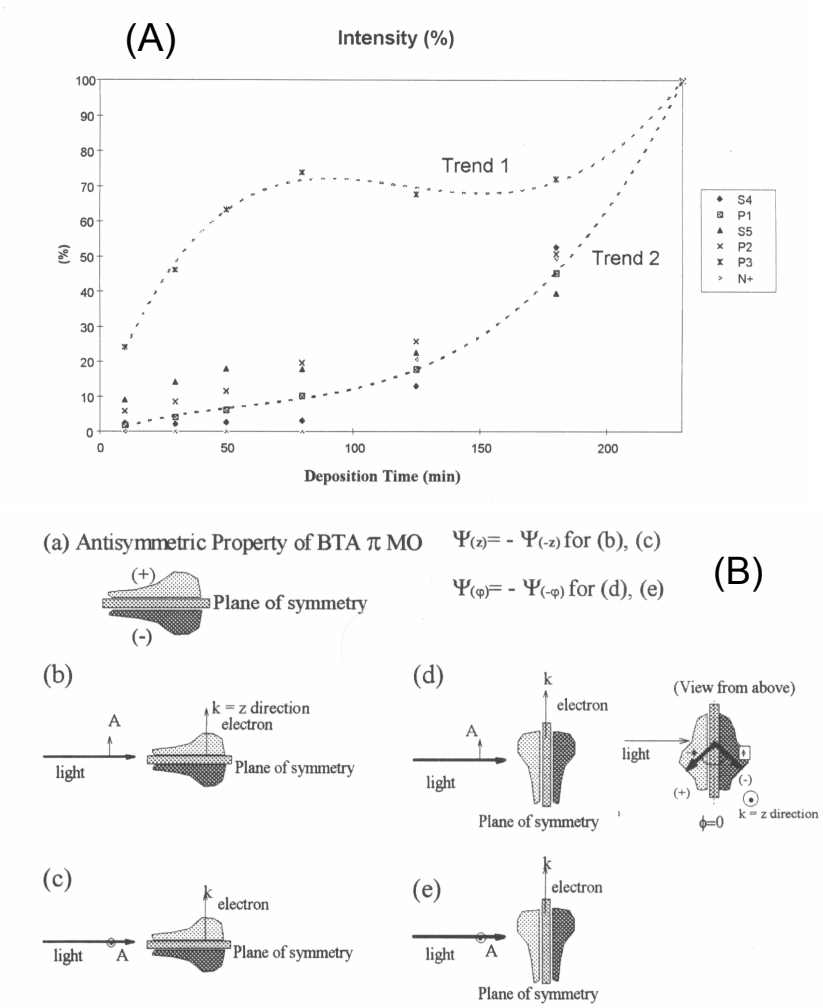

Figure 5 - (a) Relative Intensity Change and (b) Orientation of UV Polarization and BTA Molecules

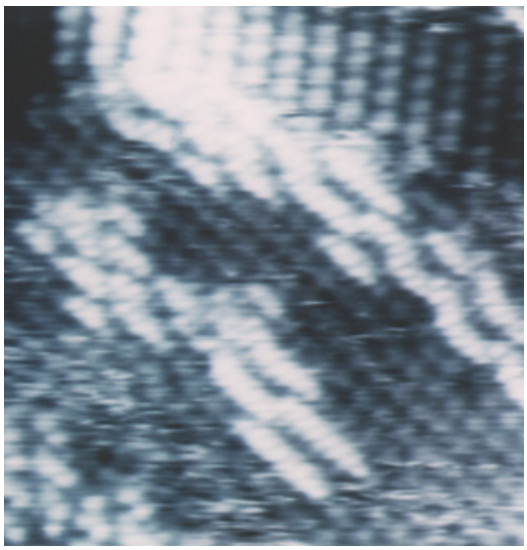

Figure 6 - STM Image of BTA layers on Cu surface, Courtesy of K. Cho and T. Sakurai[xii]

Reference

[i] G.D. Watt, R.B. Frankel, G.C. Papaefthymiou, PROCEEDINGS OF THE NATIONAL ACADEMY OF SCIENCES OF THE UNITED STATES OF AMERICA 82 (11), 3640-3643 (1985)
[ii] R.K. Watt, R.B. Frankel, G.D. Watt, Biochemistry 31 (40), 9673-9679 (1992)
[iii] R.C. Jaeger, *Introduction to microelectronic fabrication*, Modular Series on Solid State Devices Vol. 5, 2nd Ed., Prentice Hall, (2002)
[iv] A.A. Istratov, C. Flink, H. Hieslmair, E.R. Weber, T. Heiser, Phys. Rev. Lett. 81, 1243–1246 (1998)
[v] P. C. Andricacos, C. Uzoh, J. O. Dukovic, J. Horkans, and H. Deligianni, IBM Journal of Research and Development, **42** (5), http://www.research.ibm.com/journal/rd/425/andricacos.html (1998)
[vi] Y. Park, H. Noh, Y. Kuk, K. Cho, T. Sakurai, Journal of Korean Physical Society **29** (6) pp.745-749 (1996)
[vii] R.F. Roberts, Journal of Electron Spectroscopy and Related Phenomena **4**, p.273 (1974)
[viii] B.S. Fang, C.G. Olson, D.W. Lynch, Surface Science **176**, p.476 (1986)
[ix] Z. Xu, S. Lau, P.W. Bohn, Langmuir **9**, p.993 (1993)
[x] J.F. Walsh, H.S. Dhariwal, A. Gutierrez-Sosa, P. Finetti, C.A. Muryn, N.B. Brookes, R.J. Oldman, G. Thornton, Surface Science **415**, p.423 (1998)
[xi] M.H. Palmer and S.M.F. Kennedy, Journal of Molecular Structure **43**, p.203 (1978)
[xii] K. Cho, J. Kishimoto, T.Hashizume, T. Sakurai, Japanese Journal of Applied Physics Part 2-Letters **33** (1b) pp.l125-l128 (1994)